J. Chem. Thermodynamics 105 (2017) 226–237

Contents lists available at ScienceDirect

J. Chem. Thermodynamics

journal homepage: www.elsevier.com/locate/jct

Activity coefficients at infinite dilution of hydrocarbons in glycols: Experimental data and thermodynamic modeling with the GCA-EoS

Mariana González Prieto [a], Mark D. Williams-Wynn [b], Indra Bahadur [c], Francisco A. Sánchez [a], Amir H. Mohammadi [b,d,e], Selva Pereda [a,b,*], Deresh Ramjugernath [b]

[a] Planta Piloto de Ingeniería Química (PLAPIQUI-UNS-CONICET), Camino La Carrindanga Km 7, 8000 Bahía Blanca, Argentina
[b] Thermodynamics Research Unit, School of Engineering, University of KwaZulu-Natal, Howard College Campus, King George V Avenue, Durban 4041, South Africa
[c] Department of Chemistry and Materials Science Innovation & Modelling Research Focus Area, School of Mathematical and Physical Sciences, Faculty of Agriculture, Science and Technology, North-West University (Mafikeng Campus), Private Bag X2046, Mmabatho 2735, South Africa
[d] Institut de Recherche en Génie Chimique et Pétrolier (IRGCP), Paris Cedex, France
[e] Département de Génie des Mines, de la Métallurgie et des Matériaux, Faculté des Sciences et de Génie, Université Laval, Québec, QC G1V0A6, Canada

ARTICLE INFO

Article history:
Received 6 June 2016
Received in revised form 26 September 2016
Accepted 5 October 2016
Available online 6 October 2016

Keywords:
Glycols
Hydrocarbons
Infinite dilution activity coefficient
Gas-liquid chromatography
GCA-EoS

ABSTRACT

The infinite dilution activity coefficients for 12 non-polar hydrocarbon solutes in the solvents, monoethylene and diethylene glycol, were measured using the gas-liquid chromatography technique. Presaturation of the carrier gas was required to avoid solvent loss from the chromatographic column during the measurements that were carried out at T = (303.15, 313.15 and 323.15) K for monoethylene glycol and at T = (304.15, 313.15 and 323.15) K for diethylene glycol. The solutes investigated include *n*-alkanes, 1-alkenes, and cycloalkanes. The new data are compared with the highly scattered data that is available in the open literature. Finally, these highly non-ideal systems are modeled with the GCA-EoS.

1. Introduction

Due to the combination of ever-growing energy demands and decreased fossil oil resources, the oil industry has had to develop new, advanced methods to enable improvements in fuel production [1]. Physical absorption solvents are used for treating natural gas and fossil fuel streams in a number of applications, to ensure continuous and safe production. For example, glycols, such as monoethylene glycol (MEG), diethylene glycol (DEG), and triethylene glycol (TEG), are commonly used in natural gas and fossil fuel dehydration processes. Moreover, MEG is also used to prevent gas hydrate formation and DEG and TEG have, for many years, been used for the dehydration of natural gases [2].

Natural gas often contains small quantities of heavy hydrocarbons (HHCs). The presence of these HHCs can cause many operational and economic problems, such as foaming and flooding in glycol units that are used to dehydrate the natural gas. Precise design and optimization of these units requires accurate knowledge of the solubilities of the natural gas components in the glycol-aqueous solution systems. It is, therefore, necessary to rely on accurate and consistent experimental data and thermodynamic models. A literature review for the systems present in such a unit show that the available data exhibit a high degree of scatter.

Hydrocarbons show very low solubilities in glycols, and thus, their behaviour can be approximated by infinite dilution conditions. Furthermore, the infinite dilution activity coefficients are useful for the development of thermodynamic models as they provide information with regards to the solute-solvent interactions in the absence of solute-solute interactions. In this work, the infinite dilution activity coefficients of 12 hydrocarbons in MEG and DEG were measured at T = (303.15, 313.15 and 323.15) K.

Tables 1 and 2 summarise the infinite dilution activity coefficient data available in the open literature for hydrocarbons in MEG and DEG, respectively. The literature data are highly scattered, especially for the systems with MEG. In both of these tables, the temperature range, the number of measurements, the source of the data, and the reported uncertainties are provided. Unfortunately, several of the measurements were undertaken in a narrow temperature range. Moreover, many authors only reported a single activity coefficient at one temperature, which was in most cases at

* Corresponding author at: Planta Piloto de Ingeniería Química (PLAPIQUI-UNS-CONICET), Camino La Carrindanga Km 7, 8000 Bahía Blanca, Argentina.
E-mail address: spereda@plapiqui.edu.ar (S. Pereda).

http://dx.doi.org/10.1016/j.jct.2016.10.013
0021-9614/

Nomenclature

B_{11}	second virial coefficient of a pure compound
B_{12}	cross second virial coefficient of the compound (1) and the compound (2)
d_c	hard sphere diameter at the critical temperature (cm mol^{-1})
DEG	diethylene glycol
g_{ii}, g'_{ii}, g''_{ii}	group surface energy (atmcm^6 mol^{-2}) and temperature dependence
g^*_{ii}	group surface energy at reference temperature T^*
I	ionization energy
J_2^3	pressure correction term
k_{ij},k'_{ij}	group binary interaction parameters
MEG	monoethylene glycol
n_3	number of moles of the solvent
P_c	critical pressure
P_1^0	saturate vapour pressure of the solute at the temperature T
P_{in}	inlet pressure
P_0	outlet pressure
q_i	number of surface segments assigned to group i
q_{0V}	volumetric flow rate of the carrier gas
R	ideal gas constant
RI	refractive index
T	temperature
T_i^*	reference temperature of the group i (K)
T_c	critical temperature
TeEG	tetraethylene glycol
TEG	triethylene glycol
t_R	solute retention time
t_{RG}	retention time of an inert gas
V	molar volume
V_c	critical volume
V_N	net retention volume
v_1^*	molar volume of the solute
v_1^∞	partial molar volume of the solute at infinite dilution

Greek symbols

α_{ij},α_{ji}	non-randomness parameters
γ^∞	activity coefficient at infinite dilution
ε_{kilj}	cross-association energy (K)
κ_{kilj}	cross-association volume (cm^3 mol^{-1})
ρ	density
σ	collision diameter
ω	acentric factor

room temperature. In that regard, the data reported in this work contributes to understand the temperature dependence of the non-ideality of heavy *n*-alkanes, olefins and naphthenes with glycols. Moreover, up to our knowledge, this is the first time that infinite dilution activity coefficient data of 1-nonene in MEG and DEG is reported. In the case of the other hydrocarbons, the new data contribute to extend the temperature range in which they are available (see section of Results and discussion).

Gas-liquid chromatography (GLC) and inert gas stripping (IGS) were the most common techniques used to measure the infinite dilution activity coefficient of hydrocarbons in glycols by the authors referenced in Tables 1 and 2. It is important to highlight that these two methods are more precise when the solvents being investigated are non-volatile. With the more volatile solvents, solvent elution (stripped from the column by the carrier gas) is a source of systematic error. Authors that employed the GLC technique, such as Wardencki and Tameesh [3], Arancibia and Catoggio [4,5], and Williams Wynn et al. [6], pre-saturated the carrier gas before it entered the column. Similarly, in the IGS technique, the stripping gas should be saturated with the solvent before entering the equilibrium cell, in order for the mass of solvent in the cell to remain constant. In this method, the assessment of the slope of the logarithm of the solute vapour content with respect to time is the main source of uncertainty, in particular for highly immiscible systems [7]. The gas stripping technique was used by Afzal et al. [8] and Murotomi et al. [9], but only Afzal et al. saturated the stripping gas before it entered the equilibrium cell.

Castells [12] made a comprehensive review of the sources of systematic error in the determination of partition coefficients by gas chromatography. Vapour phase non-idealities, mixed retention mechanism, column hold up, and the stationary phase volume are key points that must be precisely assessed in order to avoid inaccuracies in the experimental data. In this regard, Arancibia and Catoggio [4,5], and Wardencki and Tameesh [3] neglected the non-idealities in the vapour phase. These corrections are in general low (0.2–5%) according to Castells [12]. Moreover, in their calculations of the column hold-up, Wardencki and Tameesh, as well as Arancibia and Catoggio injected methane as an inert gas. However, this gave rise to many discussions and alternative proposals [12]. A systematic error may be introduced by using methane as the inert gas, due to the solubility of the methane in the solvent and solutes. These errors are normally even larger than those resulting from the neglect of the vapour phase non-idealities [12].

The discrepancies between data reported in the literature can also be attributed to the presence of impurities in the solvent. Due to the hygroscopic nature of glycols, special care must be taken to prevent water in the air from being absorbed by the glycols. In the works of Arancibia and Catoggio [4,5], and Williams Wynn et al. [6] the solvents were degassed under vacuum prior to being used in the column prepared. In the work of Afzal et al. [8] MEG was treated with a UOP molecular sieve. Wardencki and Tameesh [3] did not perform further purification of the MEG used in their studies.

Another important issue to consider, besides solubility, is that adsorption retention mechanisms on the uncoated portions of the solid-stationary phase interface or on the gas-liquid interface could take place simultaneously with the solute partition. The first mechanism often occurs with polar solutes and can be recognized by asymmetrical output peaks from the detector. Solute adsorption at the gas-liquid interface is important in mixtures that display strong positive deviations from the ideal solution behaviour, i.e. systems displaying large infinite dilution activity coefficients. In general, this second mechanism is not directly observable; it can be inferred by calculation of the retention volumes obtained from different loadings of the stationary phase and assessing the activity coefficient by extrapolation. This experimental estimation technique is considerably less accurate than that used when no adsorption occurs. Arancibia and Catoggio stated that they obtained symmetric peaks for all measurements, indicating those experiments were conducted within the concentration range in which Henry's law applies and that the solute adsorption at the solid surface was negligible.

Headspace gas chromatography (HS-GC) is another interesting technique for measuring the activity coefficients at infinite dilution

Table 1
Experimental infinite dilution activity coefficient data of hydrocarbons in MEG available in the literature.

Solvent: MEG					
Solute	*Temperature*/K	Data points	Uncertainty	Source	Technique
n-Pentane	298.7–333.7	9	$u_r(\gamma_{i,s}^{\infty}) = 0.05$	[8]	IGS
n-Hexane	298.8–333.7	5	$u_r(\gamma_{i,s}^{\infty}) = 0.05$	[8]	IGS
	313.2–353.5	3	N/A	[9]	IGS
	298.15	1	N/A	[4]	GC
	293.15–308.15	4	$u_r(\gamma_{i,s}^{\infty}) = 0.05$	[3]	GC
	293.15	1	N/A	[10]	N/A
n-Heptane	298.7–333.7	4	$u_r(\gamma_{i,s}^{\infty}) = 0.05$	[8]	IGS
	333.15	1	N/A	[2]	N/A
	298.15	1	N/A	[4]	GC
	293.15–308.15	4	$u_r(\gamma_{i,s}^{\infty}) = 0.05$N/A	[3]	GC
n-Octane	298.7–333.7	4	$u_r(\gamma_{i,s}^{\infty}) = 0.05$	[8]	IGS
	332.1–392.4	4	N/A	[9]	IGS
	298.15	1	N/A	[4]	GC
	293.15–308.15	4	$u_r(\gamma_{i,s}^{\infty}) = 0.05$	[3]	GC
	298.15	1	N/A	[11]	HS-GC
n-Nonane	298.15	1	N/A	[4]	GC
	293.15–308.15	4	$u_r(\gamma_{i,s}^{\infty}) = 0.05$	[3]	GC
1-Hexene	293.15, 298.15	2	N/A	[4]	GC
	293.15	1	N/A	[10]	N/A
1-Heptene	298.15	1	N/A	[4]	GC
1-Octene	298.15	1	N/A	[4]	GC
Cyclohexane	298.15	1	N/A	[4]	GC
	293.15–308.15	1	$u_r(\gamma_{i,s}^{\infty}) = 0.05$	[3]	GC
	293.15	1	N/A	[10]	N/A
Methylcyclohexane	298.15	1	N/A	[4]	GC

IGS: Inert Gas Stripping, GC: Gas Chromatography, HS-GC: Headspace Gas Chromatography, and N/A: not available (the database [10] did not report the acquisition method).

Table 2
Experimental infinite dilution activity coefficient data of hydrocarbons in DEG available in the literature.

Solvent: DEG					
Solute	*Temperature*/K	Data points	Uncertainty	Source	Technique
n-Pentane	333.15–363.15	3	$u_r(\gamma_{i,s}^{\infty}) = 0.06$	[6]	GC
n-Hexane	333.15–363.15	3	$u_r(\gamma_{i,s}^{\infty}) = 0.03$	[6]	GC
	298.15	1	N/A	[5]	GC
n-Heptane	333.15–363.15	3	$u_r(\gamma_{i,s}^{\infty}) = 0.03$	[6]	GC
	298.15	1	N/A	[5]	GC
	333.15	1	N/A	[2]	N/A
n-Octane	333.15–363.15	3	$u_r(\gamma_{i,s}^{\infty}) = 0.03$	[6]	GC
	298.15	1	N/A	[5]	GC
	298.15	1	N/A	[11]	HS-GC
n-Nonane	333.15–363.15	3	$u_r(\gamma_{i,s}^{\infty}) = 0.03$	[6]	GC
	298.15	1	N/A	[5]	GC
1-Hexene	333.15–363.15	3	$u_r(\gamma_{i,s}^{\infty}) = 0.03$	[6]	GC
1-Heptene	333.15–363.15	3	$u_r(\gamma_{i,s}^{\infty}) = 0.03$	[6]	GC
	298.15	1	N/A	[5]	GC
1-Octene	333.15–363.15	3	$u_r(\gamma_{i,s}^{\infty}) = 0.03$	[6]	GC
	298.15	1	N/A	[5]	GC
Cyclopentane	333.15–363.15	3	$u_r(\gamma_{i,s}^{\infty}) = 0.03$	[6]	GC
Cyclohexane	333.15–363.15	3	$u_r(\gamma_{i,s}^{\infty}) = 0.03$	[6]	GC
	298.15	1	N/A	[5]	GC
Methylcyclohexane	298.15	1	N/A	[5].	C

GC: Gas Chromatography, HS-GC: Headspace Gas Chromatography, and N/A: not available.

or partition coefficients without adsorption influence [13], with volatile solvents [14], as is the case of glycols at high temperatures. This method was employed by Park et al. [11] to characterise binary systems of *n*-octane with MEG or DEG. The main limitation of this technique is the difficulty in obtaining precise GC calibrations for highly diluted systems. New techniques for partition coefficient measurements using headspace equipment are discussed by Ettre and Kolb [15].

In this work, the gas-liquid chromatography (GLC) technique was applied with pre-saturated carrier gas to mitigate the solvent loss from the column. In addition, following the approach of Williams-Wynn et al. [6], the retention time of a reference solute through the column was periodically measured. This enabled the mass of solvent present in the column to be monitored in real-time. Moreover, the new data is modeled with the Group Contribution with Association Equation of State (GCA-EoS).

2. Materials and experimental methods

2.1. Materials and chemicals

The solvents (MEG and DEG) were degassed for approximately 1 h in vials under vacuum, in an ultrasonic bath, at a temperature of 313 K. The purities of the solvents were verified by gas

Table 3
Suppliers, purity determination and characterisation of solvents at 101 kPa.[a]

Component	Monoethylene glycol	Diethylene glycol
Supplier	Merck KGaA	Riedel-deHaen
Supplier mass fraction purity	0.995	0.99
Peak area fractions (purity)	0.996	0.992
ρ_{meas}/(g cm^{-3})	1.1100 (298.15 K)	1.1203 (288.15 K)
ρ_{lit}/(g cm^{-3})	1.1099[b](298.15 K)	1.1207[c](288.15 K)
$RI_{meas.}$	1.4319 (293.15 K)	1.4472 (293.15 K)
$RI_{lit.}$	1.4323[b](293.15 K)	1.4472[d] (293.15 K)

[a] Standard uncertainties: $u(\rho) = 0.001$ g cm^{-3}, $u(RI) = 10^{-4}$, $u(T) = 0.01$ K, $u(P) = 1$ kPa.
[b] Zorębski and Waligóra [16].
[c] Bernal-Garcia et al. [17]
[d] Sagdeev et al. [18].

chromatography. In addition, the densities and refractive indices of the solvents were measured and compared with literature data. A Shimadzu GC-2014 gas chromatograph with a thermal conductivity detector (TCD) and a Porapak Q80/100 mesh packed column were used in this work. The oven temperature was set to 473 K, with a helium flow rate of 3.5 mL/min. The densities and the refractive indices of the solvents were measured using an Anton Paar DMA 5000 densimeter and Atago RX 7000X refractometer, respectively. Table 3 compares the measured data for the pure glycols with data reported by the suppliers, as well as values obtained from literature sources. Furthermore, the sources and mass fraction purity of all materials are listed in Table 1S in the Supplementary Material. The solutes were purchased from Sigma-Aldrich, except for n-hexane, n-octane, 1-octene and cyclohexane, which were acquired from Merck. In all cases the purity is higher than 0.99. However, the purity of the solutes is not of importance for GLC measurements, since any impurities present are separated from the solute during the gas-liquid chromatography (GLC) measurements. Moreover, the absence of significant impurity peaks during analysis verified that the solutes were of an acceptable purity. No further purification of the solutes was therefore necessary.

Chromosorb WHP 80/100 mesh, supplied by SupelCo, was used as the solid support material in this study.

3. Experimental procedure

The GLC technique, with pre-saturation of the carrier gas, was used to measure the infinite dilution activity coefficients. The experimental setup that was used in this work was that previously described by Williams-Wynn et al. [6]. A schematic of this apparatus is shown in Fig. 1. The pre-saturator unit consists of a stainless steel pre-heater coil (3 m long, 3.2 mm internal diameter) and a pre-saturation cell, which was similar in design to the dilutor cell of Richon and Renon [19]. The carrier gas enters the dilutor cell through ten 50 µm internal diameter capillaries, which are immersed in the solvent contained in this cell. The cell is filled with the solvent, leaving only a small vapour space at the top. This vapour space has the effect of preventing the liquid solvent from being entrained by the carrier gas. A silicon oil bath is used to maintain the pre-saturator unit at the operating temperature. The temperature of the silicon oil in the bath is monitored using a Pt-100 temperature probe and set to a temperature slightly above that of the GC column (approximately 1 K). This temperature was chosen so as to prevent either accumulation or elution of the solvent from the downstream GC column. A Polyscience 8206 heating circulator is used to regulate the temperature of the oil in the bath. Polyscience certified that this circulator had a stability of ±0.1 K, confirmed by measurements using the calibrated Pt-100 temperature probe.

The delivery line from the pre-saturator to the injection port of the GC is heated with a jacketed nichrome element. The temperature of the line, which is measured with a calibrated Pt-100 temperature probe, is controlled manually, using a variable voltage transformer. The temperature of this line is maintained at the temperature of the GC oven.

The GC utilised for this equipment is a Shimadzu GC-2014. The constant temperature air bath of this GC has good thermal stability, with a stated maximum deviation from the set point of 0.01 K. The GC provides the gauge pressure in the injector, with an standard uncertainty of 0.1 kPa. The outlet of the GC, which is at atmospheric pressure, was registered with a Mensor DPG 2400 digital barometer.

A 1 m section of stainless steel tubing with a 4 mm internal diameter was used to house the solvent-solid packing mixture. The Chromosorb was dried in a rotary evaporator (40 rpm) at a temperature of 313 K and under vacuum. The preparation of the GC column entails the addition of a small volume of dichloromethane to known masses of solvent and Chromosorb. The dichloromethane is utilised to ensure a uniform dispersion of the solvent onto the Chromosorb; thereafter, it is evaporated in the rotary evaporator. The solvent loading on the Chromosorb

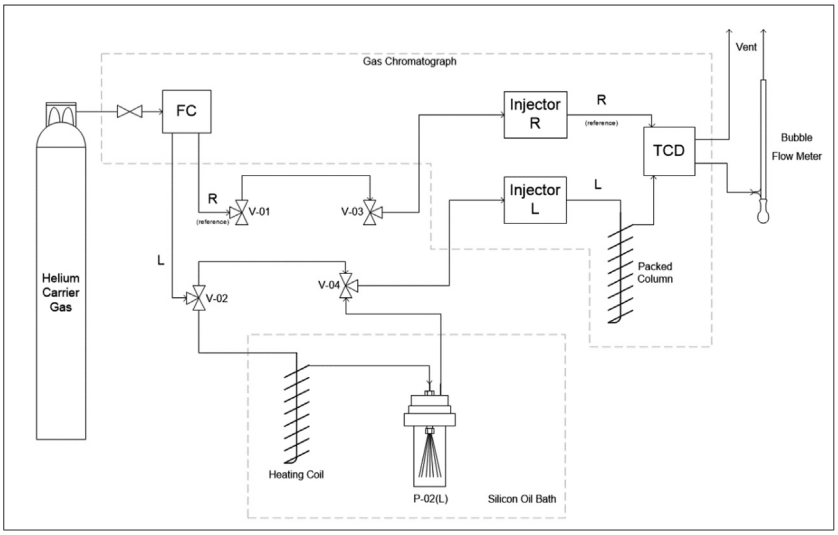

Fig. 1. Experimental apparatus for the measurement of the infinite dilution activity coefficient of organic solutes in volatile solvents. L, sample line (left); R, reference line (right); FC, flow controller; TCD, thermal conductivity detector; V-01 to V-04, three way valves 1 to 4; P-02(L), sample line pre-saturator.

Table 4
Pure component properties of the solutes studied in this work (data from Ref. [26,27]). Critical temperature, critical pressure, and critical volume (T_c, P_c, V_c), acentric factor (ω) and ionization energy (I).

Solute	T_c/K	P_c/kPa	V_c/(cm^3 mol^{-1})	ω	I/(kJ mol^{-1})
n-Pentane	469.7	3370	313	0.252	991.9
n-Hexane	507.6	3025	371	0.301	977.4
n-Heptane	540.2	2740	428	0.349	958.1
n-Octane	568.7	2490	486	0.400	945.6
n-Nonane	594.6			0.443	936.9
1-Hexene	504	3210	355	0.286	910.8
1-Heptene	537.3	2920	409	0.344	901.2
1-Octene	567	2680	468	0.392	909.9
1-Nonene	594	2330	526	0.410	908.9
Cyclopentane	511.7	4510	260	0.195	996.7
Cyclohexane	553.8	4080	308	0.208	953.3
Methylcyclohexane	572.1	3480	369	0.236	930.1

Table 5
Critical temperature (T_c) and diameter (d_c) of the solvents.

Compound	T_c[a]/K	d_c[b]/(cm mol$^{-1/3}$)
MEG	720	3.6265
DEG	753	4.5190
TEG	797	5.2044
TeEG	800	5.7790

[a] Nikitin et al. [31].
[b] Calculated from the density correlation proposed by Pereda et al. [32].

was approximately 25 wt%. The deviation of the weighted mass of solvent in the column was estimated to be 1%. After the solvent-Chromosorb mixture was packed into the stainless steel tubing, to create the GC column, it was attached in position inside of the chromatograph and conditioned by passing helium, saturated with the solvent, through the column. This was performed at the temperature at which measurements were to be undertaken, for at least half an hour, in order to remove any volatile materials remaining in the packing and to pre-saturate the column with the carrier gas. The measurements with the column were performed immediately after the conditioning was completed.

In order to achieve an approximation of infinite dilution, small volumes of the solutes of between (0.2 and 0.4) μL were injected into the column. Air was used as the inert component in this work. The average of at least three measured retention times was used for each solute. A thermal conductivity detector (TCD) was used to detect the emergence of the solutes from the column. The carrier gas flow rate was maintained at 0.5 μm^3 s^{-1} during the measurements. This was verified with a soap bubble flow meter positioned after the detector.

A reference solute (*n*-hexane) was injected at regular intervals throughout the measurements to enable the mass of solvent in the column to be monitored. The n-hexane retention time and the mass of solvent in the column were then related to one another via the *n*-hexane infinite dilution activity coefficient.

3.1. Calculation of the infinite dilution activity coefficients

The infinite dilution activity coefficients ($\gamma_{i,s}^{\infty}$) were calculated from the experimental data measured using the equation proposed by Everett [20], and improved by Cruickshank et al. [21].

$$\ln(\gamma_1^{\infty}) = \ln\frac{n_3 RT}{V_N P_1^0} - \frac{(B_{11} - v_1^*)P_1^0}{RT} + \frac{(2B_{12} - v_1^{\infty})J_2^3 P_0}{RT}, \quad (1)$$

where n_3 is the number of moles of solvent; T is the temperature of the measurement; V_N is the net retention volume; R is the gas constant; P_1^0 is the saturated vapour pressure of the solute at T; B_{11} is the second virial coefficient of the pure solute; B_{12} is the cross second virial coefficient of the solute (1) and the carrier gas (2); v_1^* is the molar volume of the solute; and v_1^{∞} is the partial molar volume of the solute at infinite dilution. v_1^* and v_1^{∞} are assumed to be equal ($v_1^* = v_1^{\infty}$). This equation is not applicable to highly polar solutes.

The equation given by Letcher et al. [22] was used to calculate the retention volume of the solute, V_N:

$$V_N = (J_2^3)^{-1} q_{0V}(t_R - t_{Rg}), \quad (2)$$

In Eq. (2), t_R is the retention time of the solute, t_{Rg} is the retention time of an inert gas and q_{0V} is the corrected volumetric flow rate of the carrier gas from the bubble flow meter.

The pressure correction term is given by Eq. (3),

$$J_2^3 = \frac{2}{3}\frac{(P_{in}/P_0)^3 - 1}{(P_{in}/P_0)^2 - 1}, \quad (3)$$

where P_{in} is the inlet pressure and P_0 is the outlet pressure. The inlet pressure is calculated as the summation of the pressure drop across the column and the atmospheric pressure.

The second virial coefficients were calculated using the correlation proposed by McGlashan and Potter [23]:

$$\frac{B}{V_c} = 0.43 - 0.886\frac{T_c}{T} - 0.694\left(\frac{T_c}{T}\right)^2 - 0.0375(N-1)\left(\frac{T_c}{T}\right)^{4.5}, \quad (4)$$

where N is the number of carbon atoms in the molecule, T_c and V_c are the critical temperature and critical molar volume of the solute, respectively.

In order to calculate the cross second virial coefficient, B_{12}, the combining rules of Hudson and McCoubrey [24], and Lorentz [25] were used to compute T_{c12} and V_{c12} from the critical properties and ionization energies of the pure components:

$$T_{c1,2} = \sqrt{T_{c1}T_{c2}}\frac{2\sqrt{I_1 I_2}}{\sqrt{I_1} + \sqrt{I_2}}2^6\frac{\sigma_1^3\sigma_2^3}{(\sigma_1 + \sigma_2)^6}, \quad (5)$$

$$\sigma_{12} = \frac{\sigma_1 + \sigma_2}{2}, \quad (6)$$

with σ being the collision diameter, which is calculated as $\sigma_i = V_{ci}^{1/3}$.

Table 4 gives the critical and physical properties of the pure component solutes used in this work. Ionization energies are reported from the Chemical Web Book of NIST [26] while the other pure component properties are those reported in the DIPPR database [27].

3.2. Thermodynamic modelling with the GCA-EoS

The Group Contribution with Association Equation of State [28,29] is an extension of the Group Contribution GC-EoS first

Table 6
GCA-EoS pure group parameters: number of surface segments (q_i), reference temperature (T_i^*), *group surface energy* (g_i^*, g_i', g_i'').

Group *i*	q_i	T_i^*/K	g_i^*/(atm cm^6 mol^{-2})	g_i'	g_i''	Correlated data
MEG	2.248	720	455519.4	−0.2135	0.0115	MEG vapour pressure [27]
CH_2OCH_2	1.32	600	406206.3	−1.0156	0.0	1,2-Dimethoxyethane and Dimethylether vapour pressure [27]

Table 7
Association parameters for the ether and alcohol groups: energy of association ($\varepsilon_{ki,lj}$) and volume of association ($\kappa_{ki,lj}$).

Site *k*	Group *i*	Site *l*	Group *j*	$\varepsilon_{ki,lj}R^{-1}$/K	$\kappa_{ki,lj}$/(cm^3 mol^{-1})	Correlated data
(−)	O	(+)	OH	2010	2.28	Excess enthalpy and VLE at 323.15 K of the binary DME + MeOH [35]

Table 8
GCA-EoS interaction parameters: group binary energy interaction (k_{ij}^*, k_{ij}') *and* non-randomness (α_{ij}, α_{ji}).

Group		k_{ij}^*	k_{ij}'	α_{ij}	α_{ji}	Correlated data
i	*j*					
MEG	CH_3	0.7882	0.0	0.0	0.0	γ^∞ of *n*-alkanes in MEG*
	CH_2	1.0715	0.0	0.0	0.0	
	CH_2 = CH	0.88	0.0	0.0	0.0	γ^∞ of 1-alkenes in MEG*
	$CyCH_2$	0.93	0.0	0.0	0.0	γ^∞ of cycloalkanes in MEG*
	CH_3cyCH_2	1.007	0.0	0.0	0.0	γ^∞ of methylcyclohexane in MEG*
CH_2OCH_2	CH_3	0.7118	0.0	0.0	0.0	$\gamma^\infty$of *n*-alkanes in DEG* and γ^∞ of *n*-alkanes in TEG [6]
	CH_2	0.9659	0.0	0.0	0.0	γ^∞ of *n*-alkanes in DEG* and γ^∞ of *n*-alkanes in TEG [6]
	CH_2OH	0.8802			0.0	γ^∞ of *n*-alkanes in DEG* and γ^∞ of *n*-alkanes in TEG [6]
	CH_2 = CH	0.765	0.0	0.0	0.0	γ^∞ of 1-alkenes in DEG*
	$CyCH_2$	0.8763	0.0	0.0	0.0	γ^∞ of cycloalkanes in DEG*
	CH_3cyCH_2	0.97	0.0	0.0	0.0	γ^∞ of methylcyclohexane in DEG*

* Data measured in this work.

Table 9
Activity coefficients at infinite dilution ($\gamma_{i,s}^\infty$) of hydrocarbons in MEG and partial molar excess enthalpy at infinite dilution (($\bar{H}_i^{E,\infty}$) at 101 kPa.[a,b]

Solute	*Temperature*/K			($\bar{H}_i^{E,\infty}$/(kJ mol^{-1})
	303.15	313.15	323.15	
n-Alkanes				
n-Pentane	$4.36{\cdot}10^2$	$3.89{\cdot}10^2$	$3.38{\cdot}10^2$	11.0
n-Hexane	$7.16{\cdot}10^2$	$6.20{\cdot}10^2$	$5.43{\cdot}10^2$	12.1
n-Heptane	$1.20{\cdot}10^3$	$1.03{\cdot}10^3$	$8.60{\cdot}10^2$	14.5
n-Octane	$1.96{\cdot}10^3$	$1.60{\cdot}10^3$	$1.34{\cdot}10^3$	16.3
n-Nonane	$2.96{\cdot}10^3$	$2.32{\cdot}10^3$	$1.97{\cdot}10^3$	17.4
1-Alkenes				
1-Hexene	$3.30{\cdot}10^2$	$2.98{\cdot}10^2$	$2.72{\cdot}10^2$	8.4
1-Heptene	$5.70{\cdot}10^2$	$5.03{\cdot}10^2$	$4.52{\cdot}10^2$	9.9
1-Octene	$9.62{\cdot}{\cdot}10^2$	$8.19{\cdot}10^2$	$7.36{\cdot}10^2$	11.5
1-Nonene	$1.61{\cdot}{\cdot}10^3$	$1.30{\cdot}10^3$	$1.17{\cdot}{\cdot}10^3$	13.6
Cycloalkanes				
Cyclopentane	$1.63{\cdot}10^2$	$1.49{\cdot}10^2$	$1.33{\cdot}10^2$	9.0
Cyclohexane	$2.70{\cdot}10^2$	$2.38{\cdot}10^2$	$2.12{\cdot}10^2$	10.4
Methylcyclohexane	$4.73{\cdot}10^2$	$4.07{\cdot}10^2$	$3.70{\cdot}10^2$	10.6

[a] Standard uncertainties: $u(T)$ = 0.1 K, $u(P)$=1 kPa, Relative combined expanded uncertainty $U_{c,r}(\gamma_{i,s}^\infty)$ = 0.03 with 0.95 level of confidence (k = 2).
[b] The standard state is the pure liquid at zero pressure as is conveniently chosen by Everett [20].

proposed by Skjold-Jørgensen [30] for associating compounds. The original model is based on the generalized van der Waals partition function and the group contribution principle. The GCA-EoS is formulated as a sum of contributions to the configurational Helmholtz free energy, A^c, as follows:

$$A^c = A^{ig} + A^{fv} + A^{att} + A^{assoc}, \quad (7)$$

where the superscripts "ig", "fv", "att" and "assoc" refer to the *ideal gas*, *free volume*, *attractive* and *association* contributions to the Helmholtz free energy, respectively. A detailed description of the model is given in the Appendix A.

Two main aspects support the use of the GCA-EoS model in this study. Firstly, the increasing number of ether groups in the glycol family makes a group contribution model an attractive alternative for prediction purposes. Secondly, the presence of oxygenated groups in glycols causes specific self-association interactions that can be correctly described by a model of the SAFT family such as the GCA-EoS. Parameters that were determined in this work are given in Tables 5–8, together with the data used for correlation. Table 5 reports critical temperature of each glycol [31] together with their critical diameter. The latter was calculated following the correlation proposed by Pereda et al. [32]. The pure group

Table 10
Activity coefficients at infinite dilution, ($\gamma_{i,s}^{\infty}$ of hydrocarbons in DEG and partial molar excess enthalpy at infinite dilution ($\bar{H}_i^{E,\infty}$) at 101 kPa.[a,b]

Solute[b]	*Temperature*/K			($\bar{H}_i^{E,\infty}$/(kJ mol^{-1})
	304.15	313.15	323.15	
n-Alkanes				
n-Pentane	$7.41 \cdot 10^1$	$7.05 \cdot 10^1$	$6.64 \cdot 10^1$	4.68
n-Hexane	$1.12 \cdot 10^2$	$1.02 \cdot 10^2$	$9.42 \cdot 10^1$	7.43
n-Heptane	$1.74 \cdot 10^2$	$1.51 \cdot 10^2$	$1.40 \cdot 10^2$	9.41
n-Octane	$2.49 \cdot 10^2$	$2.23 \cdot 10^2$	$2.03 \cdot 10^2$	8.91
n-Nonane	$3.71 \cdot 10^2$	$3.29 \cdot 10^2$	$2.95 \cdot 10^2$	9.79
1-Alkenes				
1-Hexene	$5.63 \cdot 10^1$	$5.24 \cdot 10^1$	$5.02 \cdot 10^1$	4.89
1-Heptene	$8.40 \cdot 10^1$	$7.78 \cdot 10^1$	$7.34 \cdot 10^1$	5.80
1-Octene	$1.26 \cdot 10^2$	$1.16 \cdot 10^2$	$1.08 \cdot 10^2$	6.63
1-nonene	$1.88 \cdot 10^2$	$1.74 \cdot 10^2$	$1.59 \cdot 10^2$	7.40
Cycloalkanes				
Cyclopentane	$3.38 \cdot 10^1$	$3.16 \cdot 10^1$	$3.01 \cdot 10^1$	5.08
Cyclohexane	$5.06 \cdot 10^1$	$4.67 \cdot 10^1$	$4.35 \cdot 10^1$	6.52
Methylcyclohexane	$7.72 \cdot 10^1$	$7.11 \cdot 10^1$	$6.60 \cdot 10^1$	6.78

[a] Standard uncertainties: $u(T) = 0.1$ K, $u(P) = 1$ kPa, Relative combined expanded uncertainty $U_{c,r}(\gamma_{i,s}^{\infty}) = 0.03$ with 0.95 level of confidence (k = 2).
[b] The standard state is the pure liquid at zero pressure as is conveniently chosen by Everett [20].

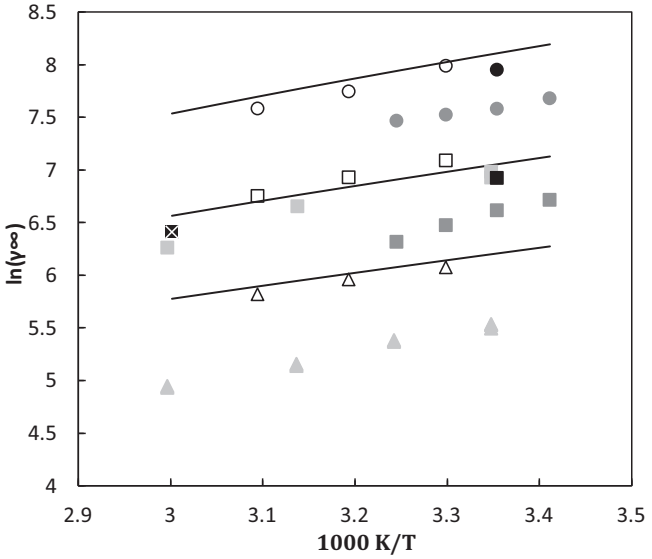

Fig. 2. Infinite dilution activity coefficients of *n*-alkanes in MEG. Symbols: experimental data for *n*-pentane (triangles), n-heptane (squares) and *n*-nonane (circles). Lines: GCA-EoS correlation. Source of experimental data: This work (○, □,△), Derawi et al. [2] (⊠), Wardencki and Tameesh [3] (●,■), Arancibia and Catoggio [4] (●,■), Afzal et al. [8] (■,▲).

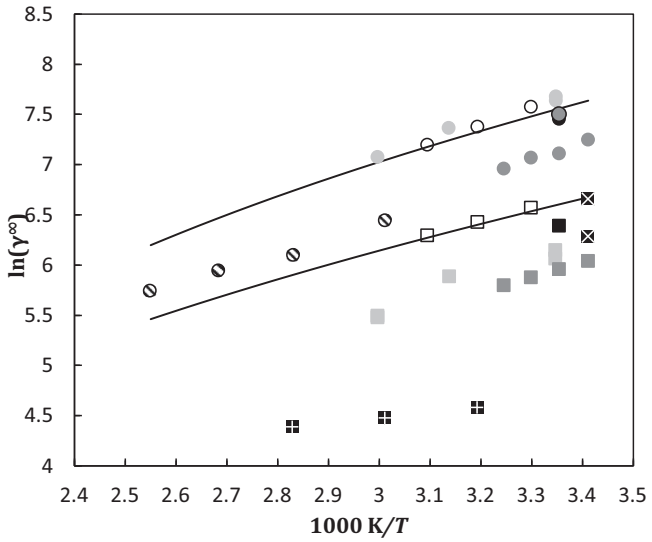

Fig. 3. Infinite dilution activity coefficients of *n*-alkanes in MEG. Symbols: experimental data for (circles) *n*-hexane and (squares) *n*-octane. Lines: GCA-EoS correlation. Source of experimental data: This work (○,□), Wardencki and Tameesh [3] (●,■), Arancibia and Catoggio [4] (●,■), Afzal et al. [8] (●,■), Murotomi et al. [9] (⊘,⊞), Dortmund Data Base [10] (⊠), Park et al. [11] (●).

surface energy parameters were obtained by correlating MEG, dimethylether (CH_3OCH_3) and 1,2-Dimethoxyethane ($CH_3OCH_2CH_2OCH_3$) vapour pressure. The first is a molecular group and the last two allow fitting the parameter of the ether group (CH_xOCH_x) without the need of binary interaction parameters. The cross-association between the ether and the hydroxyl group was determined by fitting binary data of the system dimethylether plus methanol (see Table 6). Finally, the binary energy interaction parameters reported in Table 7 were fitted to the experimental data measured in this work. Neither temperature dependence nor non-randomness parameter were required. Details about parameterization procedures can be found elsewhere [33,34].

4. Results and discussion

The $\gamma_{i,s}^{\infty}$ values obtained for each solute are given in Table 9 for MEG and in Table 10 for DEG. Each reported value was calculated based upon the average retention time of at least three experimental measurements. The uncertainty of the activity coefficient at infinite dilution is dependent upon the uncertainty of the independent variables in the equation proposed by Everett [20] and Cruickshank et al. [21], in which $\gamma_{i,s}^{\infty}$ is a function of $n_3, T, V_N, P_1^*, B_{11}, B_{12}, P_0, V_1^*, V_1^{\infty}$ and J_2^3. Thus, any uncertainty in the independent variables contributes to the uncertainty in the calculated value of $\gamma_{i,s}^{\infty}$. A detailed description of the procedure to estimate the uncertainties is given by Bahadur et al. [36]. The largest relative combined expanded uncertainties, in all cases, correspond to the measurements at the lowest temperature; although these remain less than 3%.

Figs. 2–5 show plots of the temperature dependence of the $\gamma_{i,s}^{\infty}$ for *n*-alkanes, 1-alkenes, and cycloalkanes in MEG, while Figs. 6–8 show plots of this temperature dependence in DEG. Experimental data from other sources and the GCA-EoS correlations are also included in the plots.

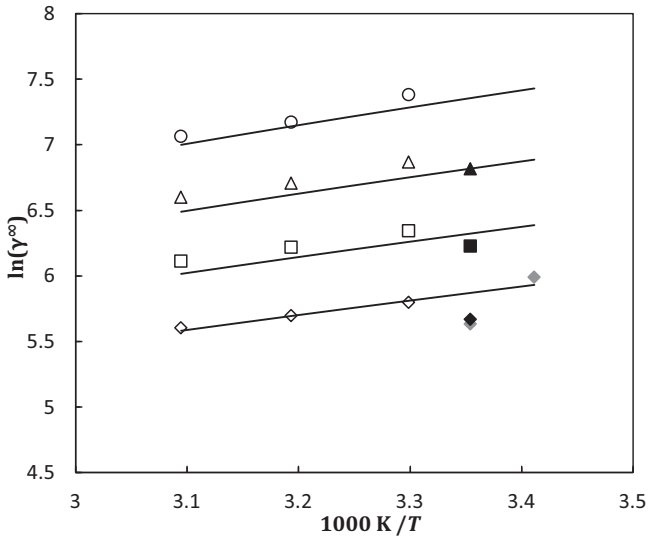

Fig. 4. Infiinite dilution activity coefficients of 1-alkenes in MEG. Symbols, experimental data for (diamonds) 1-hexene, (squares) 1-heptene, (triangles) 1-octene and (circle) 1-nonene. Lines: GCA-EoS correlation. Source of experimental data: This work (○,△,□,◇), Arancibia and Catoggio [4] (▲,■,◆), Dortmund Data Base [10] (◆).

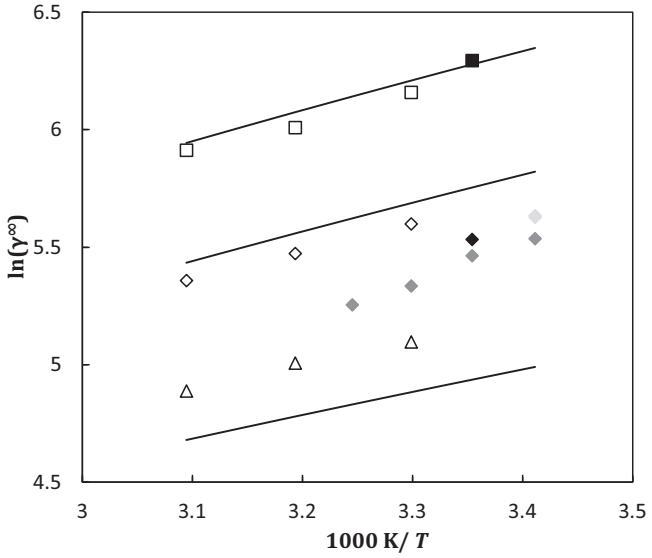

Fig. 5. Infinite dilution activity $\gamma_{i,s}^{\infty}$ coefficients of naphthenes in MEG. Symbols: experimental data for cyclopentane (triangles), cyclohexane (diamonds), methyl cyclohexane (squares). Lines: GCA-EoS correlation. Source of experimental data: this work (□,◇,△), Wardencki and Tameesh [3] (◆), Arancibia and Catoggio[4] (■,◆), Dortmund Data Base [10] (◆).

For both solvents, the general trend is that the infinite dilution activity coefficients for each solute decreases with temperature. Therefore, the solutes exhibit a positive enthalpy of mixing at infinite dilution in both MEG and DEG. In this respect, the partial molar excess enthalpy at infinite dilution can be calculated using the Gibbs-Helmholtz equation (equation 8).

$$\frac{\partial \ln(\gamma_i^{\infty})}{\partial(1/T)} = \frac{\bar{H}_i^{E,\infty}}{R}, \tag{8}$$

Tables 9 and 10 also report the molar excess enthalpy at infinite dilution for each solute-solvent pair, estimated on the basis of Eq. (8). The standard deviation of this derived property is 7.6%. As was expected, all of the hydrocarbons show a positive deviation from

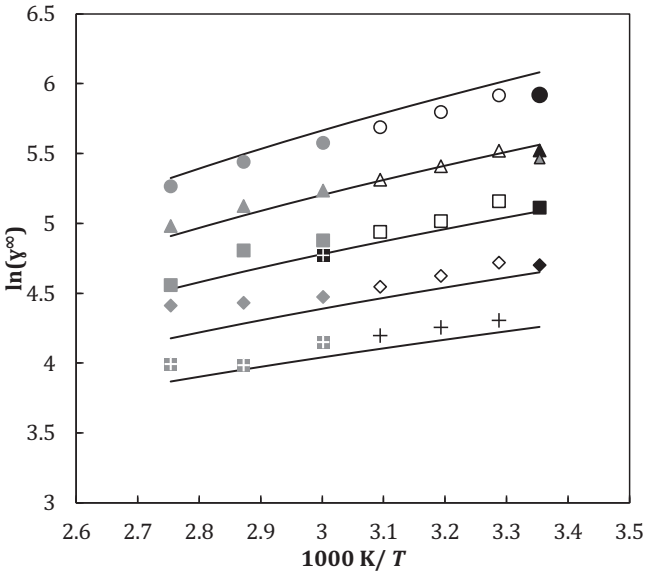

Fig. 6. Infinite dilution activity coefficients of *n*-alkanes in DEG. Symbols: experimental data for (crosses) *n*-pentane, (diamonds) *n*-hexane, (squares) *n*-heptane, (triangles) *n*-octane, and (circles) *n*-nonane. Lines: GCA-EoS correlation. Source of experimental data: this work (○,△,□,◇,+), Derawi et al. [2] (⊞), Arancibia and Catoggio [5] (●,▲,■,◆), Williams-Wynn et al. [6] (●,▲,■,◆,⊞), Park et al. [11] (▲).

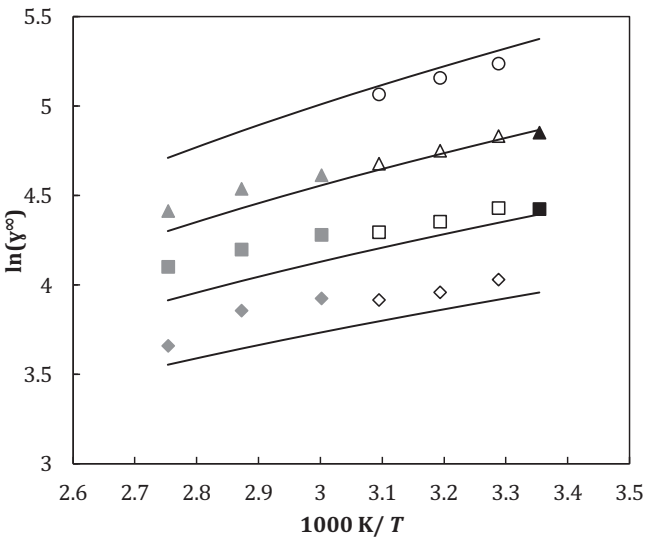

Fig. 7. Infinite dilution activity coefficients of 1-alkenes in DEG. Symbols: experimental data for 1-hexene (diamonds), 1-heptene (squares), 1-octene (triangles) and 1-nonene (circles). Lines: GCA-EoS correlation. Source of experimental data: this work (○,△,□,◇), Williams-Wynn et al. [6] (▲,■,◆), Arancibia and Catoggio [5] (▲,■).

Raoult's law in both solvents. This deviation is greater in MEG than in DEG. The less polar hydrocarbons show larger deviations. Moreover, within each homologous series of hydrocarbons, the non-ideality increases with an increase in the solute molecular weight.

As can be seen in Figs. 2 and 3, the data of *n*-alkane infinite dilution activity coefficients in MEG are very scattered. Based upon Eq. (8), a linear dependence should be found between $\ln\left(\gamma_{i,s}^{\infty}\right)$ and the reciprocal of temperature in short temperature ranges. This behavior is shown by all datasets, however, the available data show significant differences, which is more pronounce for the lighter hydrocarbons (pentane and hexane). The data measured in this

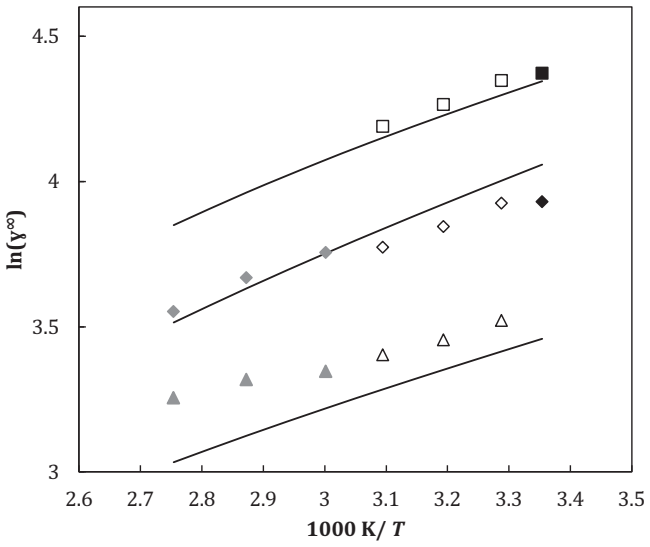

Fig. 8. Infinite dilution activity coefficients of naphthenes in DEG. Symbols: experimental data for cyclopentane (triangles), cyclohexane (diamonds) and methyl cyclohexane(squares). Lines: GCA-EoS correlation. Source of experimental data: this work (□,◇, △), Williams-Wynn et al. [6] (◆,▲), Arancibia and Catoggio [5] (▲,■).

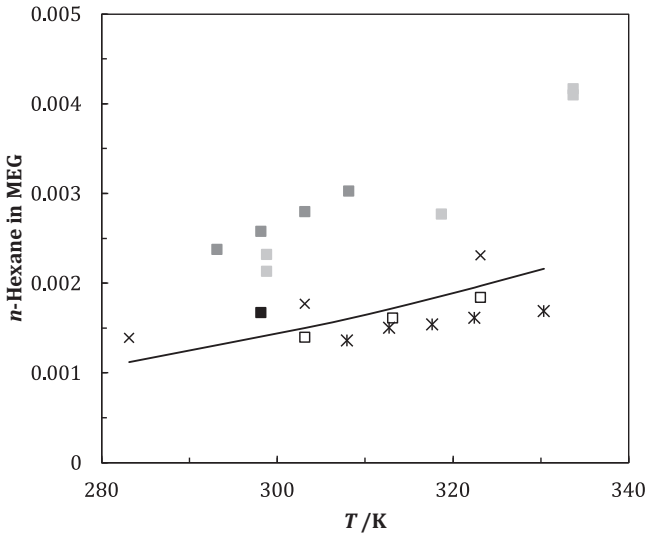

Fig. 9. Solubility of *n*-hexane in MEG from literature (stars) and its estimation as the reciprocal of infinite dilution activity coefficient data (squares). Line: GCA-EoS correlation. Source of experimental data: this work (□), Derawi et al. [37] (∗), Razzouk et al. [38] (×), Wardencki and Tameesh [3] (■), Arancibia and Catoggio [4], (■) Afzal et al.[8] (■).

work is in good agreement with that reported by Arancibia and Catoggio [4]. Also, data reported by Afzal et al. [8] of n-heptane and n-octane is in good agreement with our data; however, it is not the case for the lighter hydrocarbons, n-pentane and n-hexane. Finally, we found major differences with the data measured by Wardencki and Tameesh [3] and Murotomi et al. [9].

For solutions with high positive deviations from ideal behaviour, the solvent capacity of the solute can be approximated by $x_i = 1/\gamma^{\infty}_{i,s}$, where x_i is the molar fraction. Fig. 9 shows that the solubility of *n*-hexane in MEG, estimated based on the $\gamma^{\infty}_{i,s}$ data of this work is in good agreement with the LLE data published by Derawi et al. [37]. Similarly, Fig. 10 shows the solubility of *n*-heptane in MEG, which compares less favourably. The data from this work

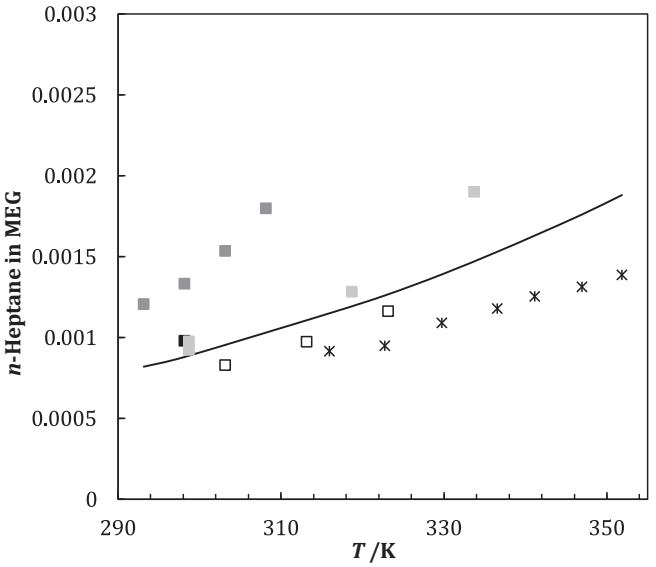

Fig. 10. Solubility of *n*-heptane in MEG from literature (stars) and its estimation as the reciprocal of infinite dilution activity coefficient data (squares). Line: GCA-EoS correlation. Source of experimental data: this work (□), Derawi et al. [37] (∗), Wardencki and Tameesh [3] (■), Arancibia and Catoggio[4] (■), Afzal et al. [8] (■).

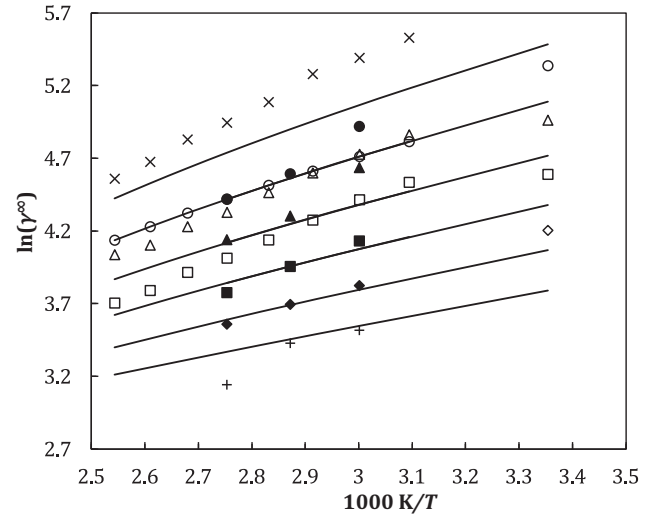

Fig. 11. Infinite dilution activity coefficient of *n*-alkanes in TEG [5,6,39]. Symbols: experimental data for (+) *n*-pentane, (◇) *n*-hexane, (□) *n*-heptane, (△) *n*-octane, (○) *n*-nonane, and (×) *n*-decane. Full symbols: data used in the model parametrization. Lines: GCA-EoS prediction.

remains nearer to the data obtained from LLE measurements than the other literature data [3,4,8].

Infinite dilution activity coefficients of the hydrocarbons studied in this work, but in binary mixtures with other glycols, like TEG and TeEG, were published by Williams-Wynn [6], Sun et al. [39], and Arancibia and Catoggio [5]. Figs. 11–13 depict GCA-EoS predictions for these binary mixtures.

5. Conclusions

In this work, new experimental infinite dilution activity coefficient data for various hydrocarbons in MEG and DEG at T = (303.15, 313.15 and 323.15) K were measured by the gas-liquid chromatography method. With both solvents, the hydrocarbons show a positive enthalpy of mixing at infinite dilution. This was calculated

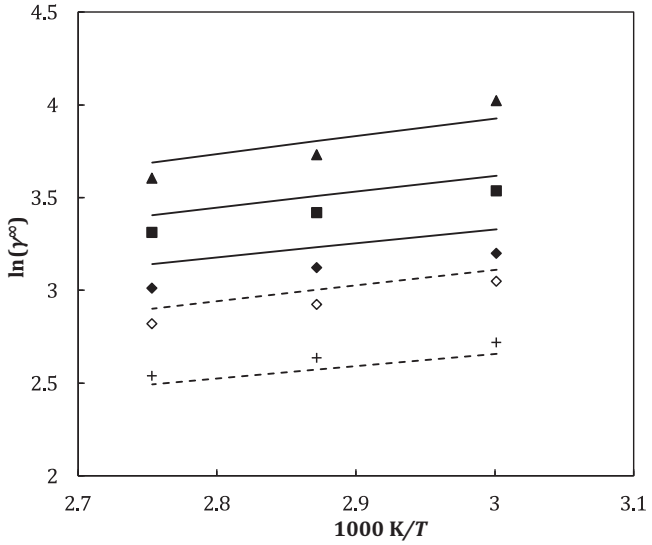

Fig. 12. Infinite dilution activity coefficient of 1-alkenes and naphthenes in TEG [6]. Symbols: experimental data for (◆) 1-hexene, (■) 1-heptene (▲) 1-octene, (+) cyclopentane, and (◇) cyclohexane. Lines: GCA-EoS predictions.

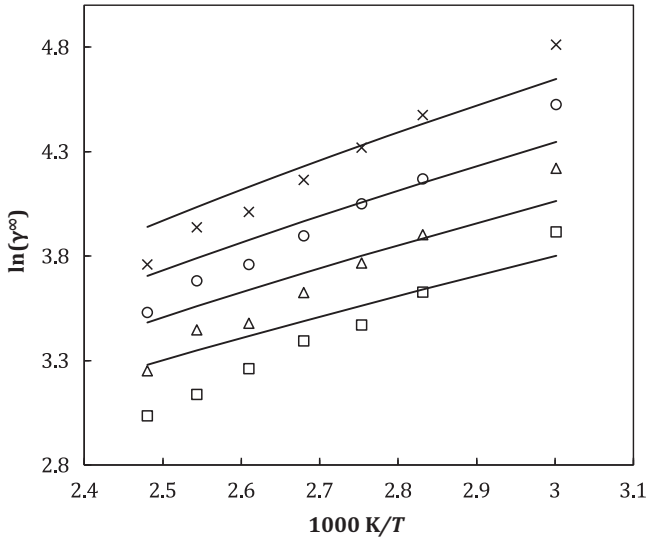

Fig. 13. Infinite dilution activity coefficient of *n*-alkanes in TeEG [39]. Symbols: experimental data for (□) *n*-heptane, (△) *n*-octane, (○) *n*-nonane, and (×) *n*-decane. Lines: GCA-EoS predictions.

using the Gibbs-Helmholtz equation. The experimental infinite dilution activity coefficients were compared to literature data, and a high degree of scatter was found for the data from various sources, especially for the $\gamma_{i,s}^{\infty}$ in MEG. The data from this study was shown to agree with LLE data obtained from literature acquired with an analytic technique. The infinite dilution activity coefficients of hydrocarbons in glycols (MEG, DEG, TEG, and TeEG) were satisfactory modeled using the GCA-EoS.

Acknowledgements

The authors are grateful to National Research Foundation (South Africa) and MinCyT (Argentina) for the financial support of this bilateral cooperation project. We also acknowledge CONICET and Universidad Nacional del Sur for the financial support.

Appendix A

A.1. The GCA-EoS thermodynamic model

There are three contributions to the residual Helmholtz energy in the GCA-EoS model: free volume, attractive and associating. The free volume and attractive contributions are based on Carnahan-Starling [40] and Non Random Two Liquids (NRTL) [41] models respectively, and keep the same formulation as in the original GC-EoS proposed by Skjold-Jørgensen [42].

The Carnahan–Starling repulsive term follows the expression developed by Mansoori et al. [43]:

$$\frac{A^{\mathrm{fv}}}{RT} = 3\frac{\lambda_1\lambda_2}{\lambda_3}(Y-1) + \frac{\lambda_2^3}{\lambda_3^2}(Y^2 - Y - \ln Y) + n\ln Y, \tag{A.1}$$

with

$$Y = \left(1 - \frac{\pi\lambda_3}{6V}\right)^{-1}, \tag{A.2}$$

$$\lambda_k = \sum_{i=1}^{NC} n_i d_i^k \quad (k = 1,2,3), \tag{A.3}$$

where n_i is the number of moles of component i, NC denotes the number of components, V represents the total volume, R denotes the universal gas constant and T is the temperature.

The following generalized expression is assumed for the hard sphere diameter temperature dependence:

$$d_i = 1.065655 d_{ci}\left[1 - 0.12\exp\left(\frac{-2T_{ci}}{3T}\right)\right], \tag{A.4}$$

where d_c is the value of the hard sphere diameter at the critical temperature, T_c, for the ith component.

The attractive contribution to the residual Helmholtz energy, A^{att}, accounts for dispersive forces between the functional groups. It is a van der Waals type of contribution, which is combined with a density-dependent local-composition expression, based on a group contribution version of the NRTL model. Upon integrating the van der Waals EoS, $A^{\mathrm{att}}(T,V)$ is equal to $-a{\cdot}n{\cdot}\rho$, with a being the energy parameter, n the number of moles and ρ the molar density. For a pure component, a is computed as follows:

$$a = \frac{z}{2}q^2 g(T), \tag{A.5}$$

where g is the characteristic attractive energy per segment and q is the number of surface segments per mole as defined in the UNIFAC model [44]. The interactions are assumed to take place through the surface of each group. The coordination number, z, is set equal to the standard value of 10. The extension of the GCA-EoS to mixtures is performed using the two fluids NRTL model, but on the basis of local surface fractions rather than local mole fractions, in a similar manner to the UNIQUAC model [45]. Therefore, the A^{att} for the mixture becomes

$$\frac{A^{\mathrm{att}}}{RT} = -\frac{\frac{z}{2}\tilde{q}^2 g_{\mathrm{mix}}}{RTV}, \tag{A.6}$$

where $\tilde{q}$ is the total number of surface segments and g_{mix} is the mixture characteristic attractive energy per total segments. These are calculated as follows:

$$g_{\mathrm{mix}} = \sum_{j=1}^{NG}\theta_j \sum_{k=1}^{NG}\frac{\theta_k \tau_{kj} g_{kj}}{\sum_{l=1}^{NG}\theta_l \tau_{lj}} \tag{A.7}$$

and

$$q = \sum_{i=1}^{NC}\sum_{j=1}^{NG} n_i v_{ij} q_j. \tag{A.8}$$

In Eq. (A.8), v_{ij} is the number of type j groups in molecule i; q_j stands for the number of surface segments assigned to group j; and θ_k represents the surface fraction of group k.

$$\theta_j = \frac{q_j}{\tilde{q}} \sum_{i=1}^{NC} n_i v_{ji}, \tag{A.9}$$

$$\tau_{ij} = \exp\left(\alpha_{ij}\frac{\tilde{q}\Delta g_{ij}}{RTV}\right), \tag{A.10}$$

$$\Delta g_{ij} = g_{ij} - g_{jj}, \tag{A.11}$$

g_{ij} stands for the attractive energy between groups i and j; and α_{ij} is the non-randomness parameter. The combination rule for the attractive energy between unlike groups is corrected by the corresponding binary interaction parameters between like groups:

$$g_{ij} = k_{ij}\sqrt{g_{ii}g_{jj}} \quad (k_{ij} = k_{ji}). \tag{A.12}$$

Furthermore, the energy and interaction parameters show the following temperature dependence:

$$g_{ii} = g_{ii}^*\left[1 + g'_{ii}\left(\frac{T}{T_i^*} - 1\right) + g''_{ii}\ \ln\left(\frac{T}{T_i^*}\right)\right] \tag{A.13}$$

and

$$k_{ij} = k_{ij}^*\left[1 + k'_{ij}\ln\left(\frac{2T}{T_i^* + T_j^*}\right)\right] \tag{A.14}$$

where g_i^* is the attractive energy and the interaction parameter at the reference temperature T_i^* and $T_i^* + T_j^*/2$, respectively.

Finally, the GCA-EoS associating contribution [29], A^{assoc}, is a group contribution version of the SAFT equation of Chapman et al. [46].

$$\frac{A^{assoc}}{RT} = \sum_{i=1}^{NGA} n_i^*\left[\sum_{k=1}^{M_i}\left(\ln X_{ki} - \frac{X_{ki}}{2}\right) + \frac{M_i}{2}\right] \tag{A.15}$$

In this equation, NGA represents the number of associating functional groups, n_i^* the total number of moles of associating group i, X_{ki} the fraction of group i non-bonded through site k, and M_i the number of associating sites in group i. The total number of moles of associating group i is calculated from v_{mi}^*, the number of associating groups i present in molecule m and the total amount of moles of specie m (n_m):

$$n_i^* = \sum_{m=1}^{NC} v_{mi}^* n_m \tag{A.16}$$

The fraction of groups i non-bonded through site k is determined by the expression:

$$X_{ki} = \left(1 + \sum_{j=1}^{NGA}\sum_{l=1}^{M_j} \frac{n_j^* X_{ki}\Delta_{ki,jl}}{V}\right)^{-1}, \tag{A.17}$$

where the summation includes all NGA associating groups and M_j sites. As can be seen, X_{ki} depends on the association strength $\Delta_{ki,lj}$:

$$\Delta_{ki,lj} = \kappa_{ki,lj}\left[\exp\left(\frac{\varepsilon_{ki,lj}}{RT}\right) - 1\right] \tag{A.18}$$

Finally, the association strength between site k of group i and site l of group j depends on the temperature T and on the association parameters $\kappa_{ki,jl}$ and $\varepsilon_{ki,jl}$, which represent the volume and energy of association, respectively.

Thermodynamic properties for evaluating phase equilibria may be derived from the configurational Helmholtz free energy, following the Maxwell relations. However, Michelsen and Hendricks [47] demonstrated that calculation of the associating contribution can be simplified by the minimization of a conveniently defined state function. Following this approach, Soria et al. [48] gave expressions for the associating contribution to the compressibility factor, Z^{assoc}, and fugacity coefficient of component j in the mixture, φ_j^{assoc}:

$$Z^{assoc} = -\frac{1}{2}\sum_{i=1}^{NGA}\sum_{k=1}^{M_i}\frac{n_i^*}{n}(1 - X_{ki}), \tag{A.19}$$

$$\ln\varphi_j^{assoc} = \sum_{i=1}^{NGA} v_{ji}^*\sum_{k=1}^{M_i}\ln X_{ki}. \tag{A.20}$$

These equations are the result of assuming a constant value for the radial distribution function in the original SAFT equation. By assuming a value of one for the radial distribution function, it was possible to take into account the association contribution by a GC approach.

Appendix B. Supplementary data

Supplementary data associated with this article can be found, in the online version, at http://dx.doi.org/10.1016/j.jct.2016.10.013.

References

[1] M. Frost, G.M. Kontogeorgis, E.H. Stenby, M.A. Yussuf, T. Haugum, K.O. Christensen, E. Solbraa, T.V. Løkken, Fluid Phase Equilib. 340 (2013) 1–6.
[2] S.O. Derawi, M.L. Michelsen, G.M. Kontogeorgis, E.H. Stenby, Fluid Phase Equilib. 209 (2003) 163–184.
[3] W. Wardencki, A.H.H. Tameesh, J. Chem. Technol. Biotechnol. 31 (1981) 86–92.
[4] E.L. Arancibia, J.A. Catoggio, J. Chromatogr. A 238 (1982) 281–290.
[5] E.L. Arancibia, J.A. Catoggio, J. Chromatogr. 197 (1980) 135–145.
[6] M.D. Williams-Wynn, T.M. Letcher, P. Naidoo, D. Ramjugernath, J. Chem. Thermodyn. 65 (2013) 120–130.
[7] D. Richon, Rev. Sci. Instrum. 82 (2011) 025108.
[8] W. Afzal, M.P. Breil, P. Théveneau, A.H. Mohammadi, G.M. Kontogeorgis, D. Richon, Ind. Eng. Chem. Res. 48 (2009) 11202–11210.
[9] A. Murotomi, M. Yokota, K. Fukuchi, Y. Iwai, Fluid Phase Equilib. 357 (2013) 24–29.
[10] Free data from Dortmund Data Bank, <http://www.ddbst.com/en/EED/ACT/ACTindex.php#1,2-Ethanediol> (accessed April 07, 2015).
[11] J.H. Park, A. Hussam, P. Couasnon, D. Fritz, P.W. Carr, Anal. Chem. 59 (1987) 1970–1976.
[12] R.C. Castells, J. Chromatogr. A 1037 (2004) 223–231.
[13] C.B. Castells, D.I. Eikens, P.W. Carr, J. Chem. Eng. Data 45 (2000) 369–375.
[14] A. Hussam, P.W. Carr, Anal. Chem. 57 (1985) 793–801.
[15] B. Kolb, L.S. Ettre, Static Headspace-Gas Chromatography: Theory and Practice, second ed., 2006.
[16] E. Zorębski, W. Agnieszka, J. Chem. Eng. Data 53 (2008) 591–595.
[17] J.M. Bernal-García, A. Guzmán-López, A. Cabrales-Torres, V. Rico-Ramírez, G.A. Iglesias-Silva, J. Chem. Eng. Data 53 (2008) 1028–1031.
[18] D.I. Sagdeev, M.G. Fomina, G.K. Mukhamedzyanov, I.M. Abdulagatov, Fluid Phase Equilib. 315 (2012) 64–76.
[19] D. Richon, H. Renon, J. Chem. Eng. Data 25 (1980) 59–60.
[20] D.H. Everett, Trans. Faraday Soc. 61 (1965) 1637.
[21] A.J.B. Cruickshank, M.L. Windsor, C.L. Young, Proc. R. Soc. A Math. Phys, Eng. Sci. 295 (1966) 259–270.
[22] T.M. Letcher, R.A. Harris, D. Ramjugernath, J.D. Raal, J. Chem. Thermodyn. 33 (2001) 1655–1662.
[23] M.L. McGlashan, D.J.B. Potter, Proc. R. Soc. A Math. Phys. Eng. Sci. 267 (1962) 478–500.
[24] G.H. Hudson, J.C. McCoubrey, Trans. Faraday Soc. 56 (1960) 761.
[25] J.R. Conder, C.L. Young, Physiochemical Measurements by Gas Chromatography, Wiley, Chichester, 1979.
[26] Chemical Web Book NIST, (2011). <http://webbook.nist.gov/chemistry/> (accessed April 07, 2015).
[27] DIPPR801-Database, Thermophys. Prop. Database. (1998).
[28] M.S. Zabaloy, G.D.B. Mabe, S.B. Bottini, E.A. Brignole, Fluid Phase Equilib. 83 (1993) 159–166.
[29] H.P. Gros, S.B. Bottini, E.A. Brignole, Fluid Phase Equilib. 116 (1996) 537–544.
[30] S. Skjold-jørgensen, Ind. Eng. Chem. Res. 27 (1988) 110–118.
[31] E.D. Nikitin, P.A. Pavlov, A.P. Popov, J. Chem. Thermodyn. 27 (1995) 43–51.
[32] S. Pereda, S. Raeissi, A.E. Andreatta, S.B. Bottini, M. Kroon, C.J. Peters, Fluid Phase Equilib. 409 (2016) 408–416.

[33] M. González Prieto, F.A. Sánchez, S. Pereda, J. Supercrit. Fluids 96 (2015) 53–67.
[34] M.G. Prieto, F.A. Sánchez, S. Pereda, Ind. Eng. Chem. Res. 54 (2015) 12415–12427.
[35] S. Park, K. Han, J. Gmehling, J. Chem. Eng. Data 52 (2007) 230–234.
[36] I. Bahadur, B.B. Govender, K. Osman, M.D. Williams-Wynn, W.M. Nelson, P. Naidoo, D. Ramjugernath, J. Chem. Thermodyn. 70 (2014) 245–252.
[37] S.O. Derawi, G.M. Kontogeorgis, E.H. Stenby, T. Haugum, A.O. Fredheim, J. Chem. Eng. Data 47 (2002) 169–173.
[38] A. Razzouk, R.A. Naccoul, I. Mokbel, P. Duchet-Suchaux, J. Jose, E. Rauzy, C. Berro, J. Chem. Eng. Data 55 (2010) 1468–1472.
[39] P. Sun, G.-H. Gao, H. Gao, J. Chem. Eng. Data 48 (2003) 1109–1112.
[40] N.F. Carnahan, J. Chem. Phys. 51 (1969) 635.
[41] H. Renon, J.M. Prausnitz, AIChE J. 14 (1968) 135–144.
[42] S. Skjold-Jørgensen, Fluid Phase Equilib. 16 (1984) 317–351.
[43] G.A. Mansoori, N.F. Carnahan, K.E. Starling, T.W. Leland Jr., J. Chem. Phys. 54 (1971) 1523–1525.
[44] A. Fredenslund, R.L. Jones, J.M. Prausnitz, AIChE J. 21 (1975) 1086–1099.
[45] D.S. Abrams, J.M. Prausnitz, AIChE J. 21 (1975) 116–128.
[46] W.G. Chapman, K.E. Gubbins, G. Jackson, M. Radosz, Ind. Eng. Chem. Res. 29 (1990) 1709–1721.
[47] M.L. Michelsen, E.M. Hendriks, Fluid Phase Equilib. 180 (2001) 165–174.
[48] T.M. Soria, A.E. Andreatta, S. Pereda, S.B. Bottini, Fluid Phase Equilib. 302 (2011) 1–9.

JCT 16-447